Ho Chong Lee
Hi Dong Chai

Integral Point-Matching Method for Two-Dimensional Laplace Field Problems with Periodic Boundaries

An integral point-matching technique is applied to two-dimensional Laplacian fields between periodic boundaries. This formulation leads to an algorithm that reduces the size of the matrix, economizing on computer workspace and inversion time. Several example problems solved on an APL terminal system are included.

Introduction

Extensive literature exists on various techniques for field computations which are associated with the equations of Laplace and Poisson. For example, in a recent group of papers devoted to LSI packaging analyses, a survey was included on computational techniques as applied to the field problems in integrated circuits [1]. In addition to wide coverage in the bibliography of this paper, some topics included in the same issue are finite element methods [2] and matrices resulting from symmetric field problems [3]. Elsewhere [4], reviews and comparisons are made among various algorithms used in direct methods. In the finite difference methods, the partial differential equations are solved on subsectioned networks of regular and irregular regions [5, 6]. Similarly, in finite element methods the field must be discretely lumped in grids and nodal points so that the conservation laws can be applied at each nodal point [2]. All of the grid information is a part of the data to be handled in the numerical computations.

In another approach, integral equations, instead of partial differential equations, may be used to develop numerical techniques [7, 8]. The integrands of these equations consist of known kernels and generally unknown source charges; determination of the source charges is the essential part of the numerical solutions.

In the absence of distributed sources (or charges) in a field with known boundary conditions (the Laplace problem), the only source charges to be determined are boundary charges. Therefore, in an integral method, only sectioned parts are the boundaries, regardless of the field size. This means far less data need be handled in computation compared to either the finite difference method or finite element method. This makes the integral methods attractive for small computer systems including interactive terminals which offer smaller storage capacities but almost instant turnaround output.

In practical situations, many field problems involve lengthy boundaries that are periodic, such as magnetic fields between toothed poles of stepping motors [9] and electric fields between conductors regularly spaced in integrated circuit boards. If, in a straightforward manner, enough periods are to be taken in the analysis so that end points do not affect central periods, a large number of elements would be required, resulting in a large matrix.

A better approach is to incorporate the periodic nature of the solution into the formulation and reduce the resulting matrix corresponding to one period of the boundary. This not only facilitates use of an interactive terminal but also gives more accurate results, making the technique also suitable for medium-size computers. Basically, there are two approaches to take. In the first, only one period is taken in the integral formulation. Since the ends of this period must be included in the closed path of the line integral, this results in added boundaries to be sectioned, and therefore added conditions (which are periodicity

conditions). In the second approach, general formulations are carried out to many periods. And then, periodic conditions are imposed on the surface charges. This avoids introducing fictitious boundaries and results in a reduced matrix size corresponding to the number of elements in one period without end lines.

In this paper, the previously mentioned more general formulations [10] are modified for such special applications to achieve reductions in data and in required storage capacity. Several examples are presented to indicate the usefulness of the formulation.

Formulation

There are several known approaches for numerical solutions of integral equations [7, 8]. For Laplace problems, the methods essentially determine the surface charges from the boundary conditions [10]. In one method, the surface charge in each sectioned boundary element is assumed constant over the element. This allows for each integration to be carried out on the kernels only over the small element. Then, these unknown surface charges, each representing an average value over the respective element, are determined through matrix inversion. The detailed general formulation is provided in Appendix A. In this section, an extension to periodic boundaries is discussed.

Figure 1 shows a field between periodic boundaries. The two opposing boundaries may not be similar and may not have a vertical line about which the field and boundaries are symmetric. But we assume that there is a common periodicity, P, so that the solution also has the common period, P. The ends of boundaries may meet to form a field between two loops, as in motors, or ends may extend to infinity, in which case the ends are regarded as joined at infinity.

A straightforward computational technique to solve periodic boundaries requires that we take several periods for computation. Then we use the solution of the central periodic section, which is least influenced by the end points. For simple geometries this technique may be satisfactory. However, for many practical geometries, the technique requires a large number of data points. As a result, it requires much computation time, even with a large computer system. Also, the accuracy of the data becomes questionable due to round-off errors and the effects of the end-point sources, which are usually large.

We avoid the above problems by making use of the periodicity of the boundary sources and boundary conditions. Returning to Fig. 1, let us designate the periodic sections by $P_0, P_{\pm 1}, P_{\pm 2} \cdots$, with P_0 being the central one.

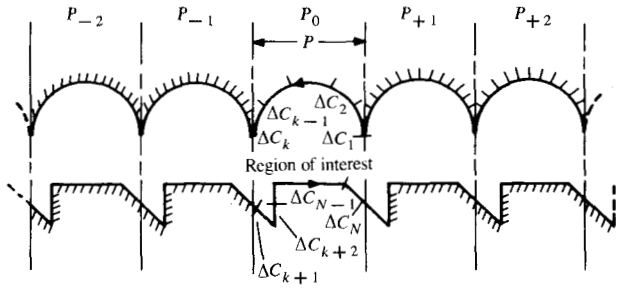

Figure 1 Periodic boundaries.

Positive subscripts indicate those sections to the right of the central section; negative subscripts indicate those to the left. In each period, the boundaries are divided into N sections $\Delta C_1, \Delta C_2, \cdots, \Delta C_N$, of which some ($\Delta C_1, \cdots, \Delta C_k$) are on one side and the others ($\Delta C_{k+1}, \cdots, \Delta C_N$) on the opposite boundary. Note that it is not necessary to have an equal number of sections on both boundaries.

We note that the boundary conditions are periodic with common period, P, so that the solution is also periodic. This means that values of α_i, β_i, and γ_i of Eqs. (A12) and (A13) of Appendix A in period P_0 repeat the patterns in all other periods. More significantly, the boundary sources σ_i in P_0 also repeat the pattern in other periods. Therefore,

$$\sigma_i^{(0)} = \sigma_i^{(\pm 1)} = \sigma_i^{(\pm 2)} = \cdots \qquad i = 1, 2, \cdots N, \tag{1}$$

where the superscripts designate the periodic sections.

It can be easily shown that the N independent equations for σ are, from (A14) and (A16),

$$\sum_{j=1}^{N} \left[\sum_{m=0,\pm 1,\pm 2,\cdots}^{\infty} \ell_{ij}^{(m)} \right] \sigma_j = \gamma_i \qquad i = 1, 2, \cdots, N, \tag{2}$$

where, from (A21),

$$\ell_{ij}^{(0)} = \ell\{\hat{z}_i;\, z_j,\, z_{j+1}\},$$

$$\ell_{ij}^{(m)} = \ell\{\hat{z}_i;\, z_j + mP,\, z_{j+1} + mP\},$$

$$i, j = 1, 2, \cdots, N,$$

$$m = 0, \pm 1, \pm 2, \cdots, \pm M, \cdots. \tag{3}$$

Thus, the matrix is reduced from the size of many periods to that corresponding to one period. Note that once the matrix elements $\ell_{ij}^{(0)}$ corresponding to the central section P_0 have been computed, subsequent matrix elements $\ell_{ij}^{(m)}$ follow immediately with translation of z_j and z_{j+1} by mP. In particular, if boundaries are periodic in the x coordinate, only x_j and x_{j+1} are translated by mP, which are real components of z's.

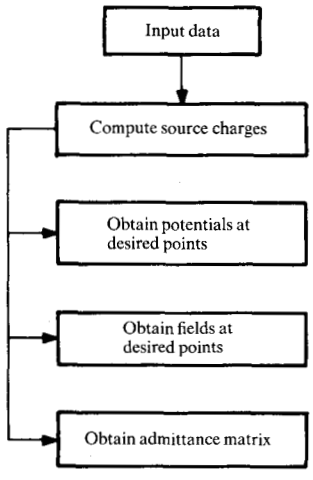

Figure 2 Program flow diagram.

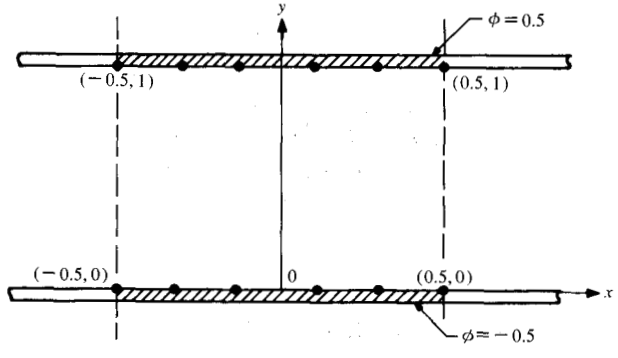

Figure 3 Parallel plate capacitor.

Although in Eq. (2) the inner summation is shown to extend to infinity, in practice a finite sum is sufficient. The terms with nonzero integers of the sum index, m, represent effects of charges placed outside the central period. Thus, the higher the integer, the lower the value of the terms, and the summation may be terminated at a reasonable number. A practical way of determining this terminal integer, of course, is to check the incremental change with a stepped summation. It is noted that the size of the summation does not affect the matrix size and has no effect on the inversion time.

It is also noted that these effects of charges outside the central period can be eliminated by introducing boundary lines on both ends of the central period. The equivalent charge distributions are obtained by imposing on these boundaries the periodic (or matching) potentials and derivatives. The charge equation corresponding to Eq. (2) takes the form

$$\sum_{j=1}^{N+2K} \ell_{ij}\sigma_j = \gamma_i \qquad i = 1, 2, \cdots, N, \tag{4}$$

$$\left.\begin{aligned} \sum_{j=1}^{N+2K} \ell'_{ij}\sigma_j &= 0 \\ \sum_{j=1}^{N+2K} \ell''_{ij}\sigma_j &= 0 \end{aligned}\right\} \quad i = N+1, N+2, \cdots, N+2K, \tag{5}$$

$$\ell_{ij} = \ell^{(0)}_{ij},$$

$$\ell'_{ij} = \bar{\Psi}_j(\hat{z}_i) - \bar{\Psi}_j(\hat{z}_{i+K}),$$

$$\ell''_{ij} = \frac{\partial\bar{\Psi}_j}{\partial n}(\hat{z}_i) - \frac{\partial\bar{\Psi}_j}{\partial n}(\hat{z}_{i+K}),$$

where K is the number of sections in each of the end lines and in Eq. (5) indices j and $j + K$ designate the corresponding elements facing each other having common potential and derivative due to the periodicity. Note that this yields a matrix size larger than that of Eq. (2) by $2K$.

Once boundary charges, σ's, are determined, (A7) through (A10) are used to compute field quantities, where the summation integer extends to all charges inside and outside the central periods. Again, in these computations, the summation would be truncated at the reasonable distances as the following examples will show.

Examples

In order to demonstrate significant features, the method developed in the previous two sections was programmed using APL [11]. The program flow is shown in Fig. 2. First the computer terminal requests input data: boundary points and boundary conditions. The input data are used to solve for sources, σ's (A23). With the knowledge of source values, we are then able to determine potential and field quantities at any specified point using Eqs. (A7)–(A10).

• *Example 1: a parallel plate capacitor*

Figure 3 shows a section of an infinitely large parallel plate capacitor. This example was chosen because its solutions are well known, enabling us to gain insight into the simplicity of data input and the rate of convergence.

We consider the plate to consist of infinite numbers of periodic sections of the unit element shown in Fig. 3. We want to find out how many such elements are required to obtain reasonably accurate results. For the example, the unit element was divided into ten equal segments (five on the top plate and the other five on the lower plate). There-

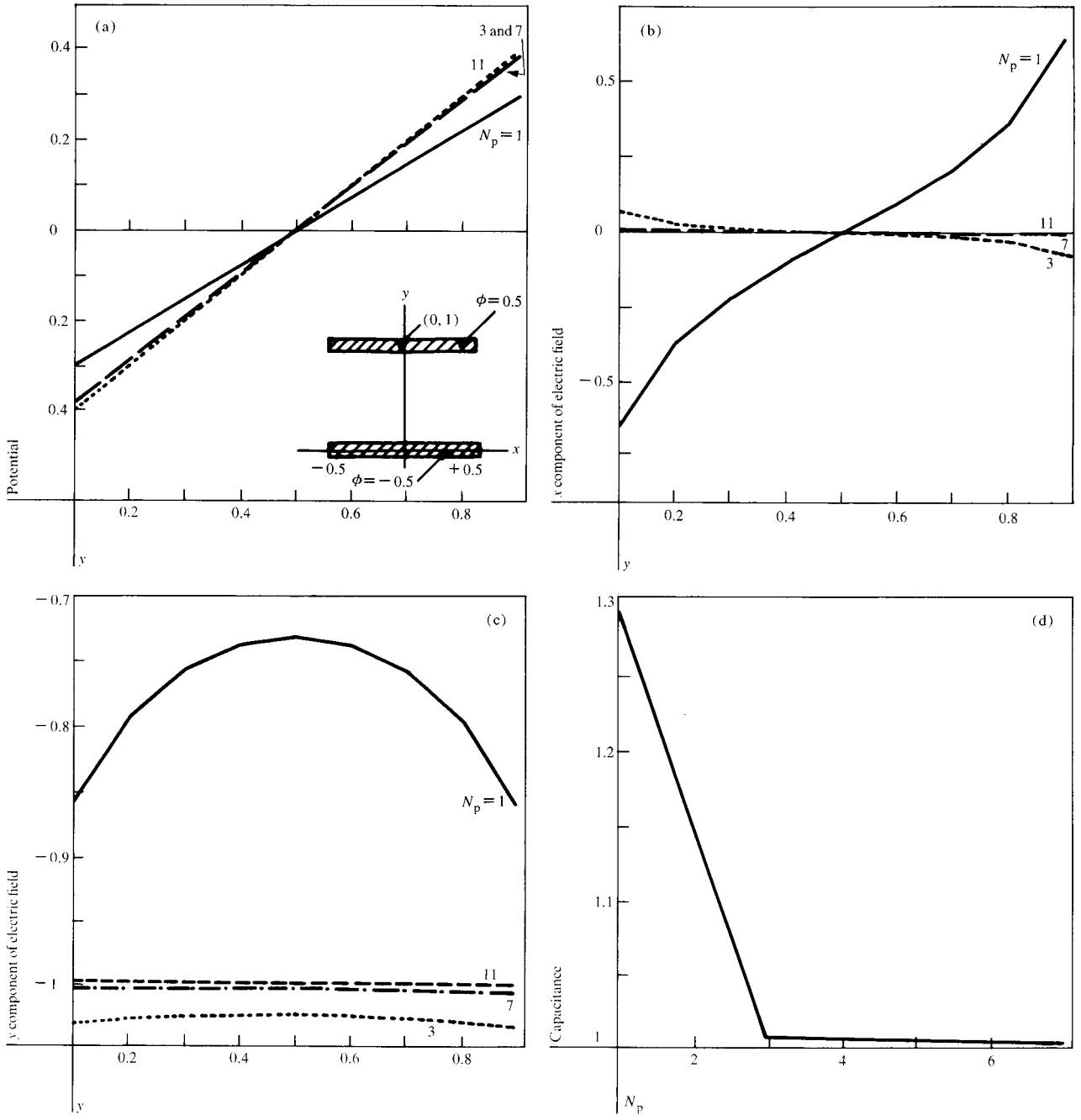

Figure 4 (a) Potential distribution along $x = 0.5$ of parallel plate capacitor (Fig. 3) with various numbers of elements in unit length (period). (b) Electric fields $\partial\phi/\partial x$ along $x = 0.5$ of parallel plate capacitor. (c) Electric field $\partial\phi/\partial y$ along $x = 0.5$ of parallel plate capacitor. (d) Capacitance of parallel plate capacitor as a function of element numbers in unit length (period).

fore, only 12 coordinate points, 10 boundary values and a little other input information, are entered into the computer. The top plate is set at a potential of 0.5 unit and the lower plate at −0.5 unit.

In Figs. 4(a), (b), and (c) we show values for potential and electric fields at $x = 0.5$ as a function of the number of periods, N_p, used in the computation. This line is chosen because this is the worst-case situation. In Fig. 4(a) the

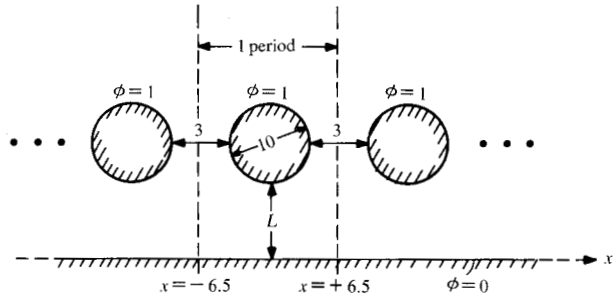

Figure 5 Cylindrical conductors above ground plane.

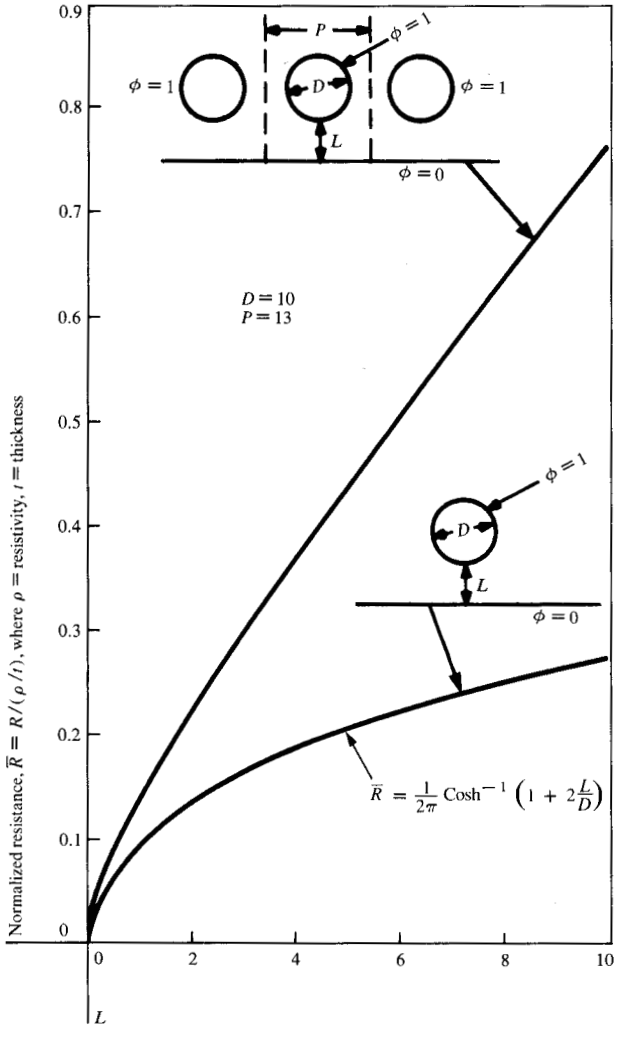

Figure 6 Effect of ground-conductor separation (L).

deviation of potential is significant with the central period only ($N_p = 1$ or $M = 0$), which is the condition for a finite plate. However, with increasing N_p the potential value quickly converges to the true one ($\phi = y - 0.5$). Figures 4(b) and 4(c) show the x and y components of the electric field. As can be seen, the convergence is not as rapid as in the case for the potential. This is expected since the electric field is a potential gradient. For N_p greater than 7, both components approach the true values ($E_x = 0$ and $E_y = -1$).

For the potential as well as the electric fields, the accuracy is poorer near sources. This is so because the source at each segment is assumed to be constant instead of a continuously varying value. Therefore, we expect that field values will be more sensitive to approximations near the boundaries. Figure 4(d) shows the capacitance of the unit element as a function of N_p. The capacitance converges rapidly to the true one ($C = 1$). With N_p equal to only 3 elements, the capacitance deviates from 1 by less than 0.007.

• *Example 2: resistance calculation*

Figure 5 shows a series of cylindrical conductors above a ground plane. Both the conductors and the ground are placed in a resistive medium. We want to compute the resistance between one of the conductors and the ground when a unit potential is applied to all of the conductors. We also want to find out the effect of the conductor-ground separation on the resistance.

A straightforward conventional approach requires that at least three conductor boundaries and a section of the ground above the three conductors be used in the computation. Then the resistance of the center conductor (defined here as the inverse of the net current flow from the conductor) must be computed. Obviously, this approach requires a large number of boundary points resulting in a large matrix for inversion. Also, the accuracy of the resulting solution is open to question.

Using the technique presented in this paper, however, the number of boundary points required is significantly reduced since we need to specify the boundary points of only one period. Therefore, our technique enables problems of this complexity to be solved with a smaller computer workspace. Also, the data input becomes simpler, making it more attractive to users.

Figure 6 shows the effect of ground-conductor separation (L) on the resistance. For L greater than 1, the resistance is very much a linear function of L. Its value is significantly different from that of a single conductor above a ground plane, the solution for which is well known. If we had used the latter value to approximate the periodic problem discussed in the example, there would have been a serious error.

A feature of our technique is that once the source charge is obtained, field parameters are easily obtained by simple computation. Figure 7 shows the current density distribution around the conductor with L equal to 3. This is obtained using Eq. (A10).

For this example, we have divided the ground plane and conductor into 26 and 40 equal segments, respectively, resulting in a matrix size of 66 by 66. Eleven periods are used for the computation, and the CPU time to obtain the source charges was 58 seconds with the IBM System/370 VM/168 system.

Discussion

As the previous examples have demonstrated, the APL algorithm in conjunction with the computational method presented in this paper provides a convenient means to solve many practical periodic boundary problems of arbitrary geometry. The algorithm is interactive, and the amount of input data is small since only boundary points and boundary conditions need be specified. It can handle multiple boundaries which are either closed or open. Since the boundaries of only one period have to be entered, the size of matrix to be solved is significantly reduced.

Although the examples presented happen to be symmetric as well as periodic, symmetry is not prerequisite for the present formulation. Figures 8 and 9 show a modified conductor and a step-motor configuration showing asymmetries. If, as an alternative to this method, only one period is used in the formulation, additional side boundaries must be introduced with periodic conditions. As shown in Eqs. (4) and (5), this increases the matrix size and introduces errors near the ends. Our present formulation circumvents such difficulties.

The amount of workspace required to invert a matrix of size N is about 25 N^2. Therefore, the reduction of the boundary points by a factor of 3 implies an order of magnitude reduction in matrix size. Therefore, the CPU time is considerably less, and the workspace size requirement is less severe. We have found that many practical problems could be solved using less than 100 boundary segments with satisfactory results. Unfortunately, in order to invert a matrix of this size, the active workspace still has to be at least 250K bytes. This limits the technique to only those who have access to large computers. However, with the accelerating computer technology, more people will be able to afford or to access a large system in the future.

The graph in Fig. 10 shows some indication of the CPU time required to obtain source charges for a given number

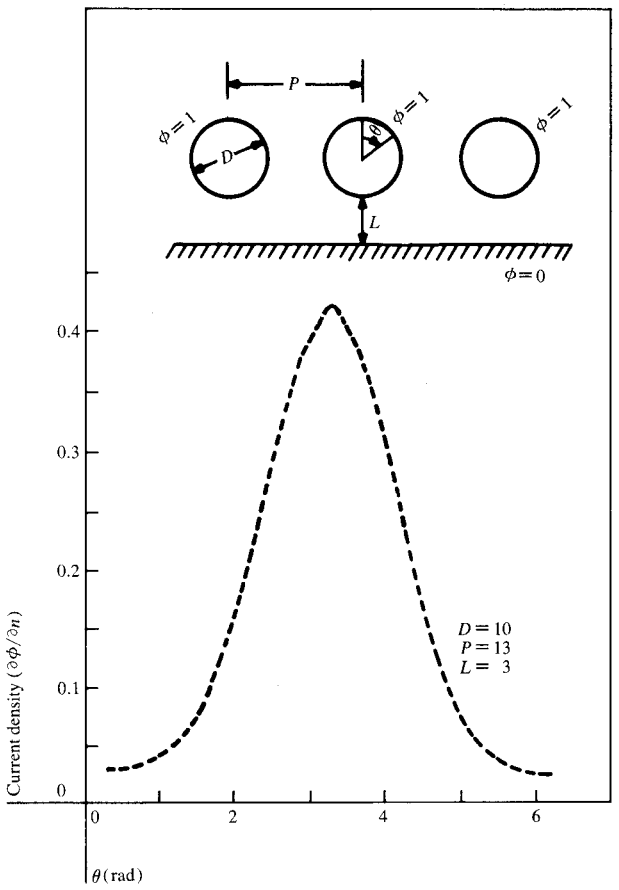

Figure 7 Current density distribution around conductor.

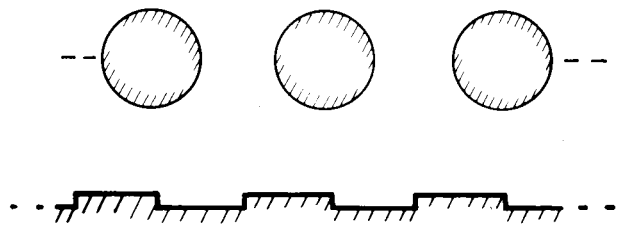

Figure 8 Cylindrical conductors above uneven ground plane.

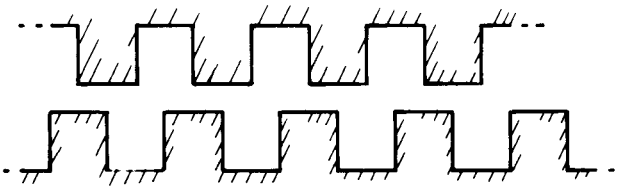

Figure 9 Stepping motor teeth at nonsymmetric displacement.

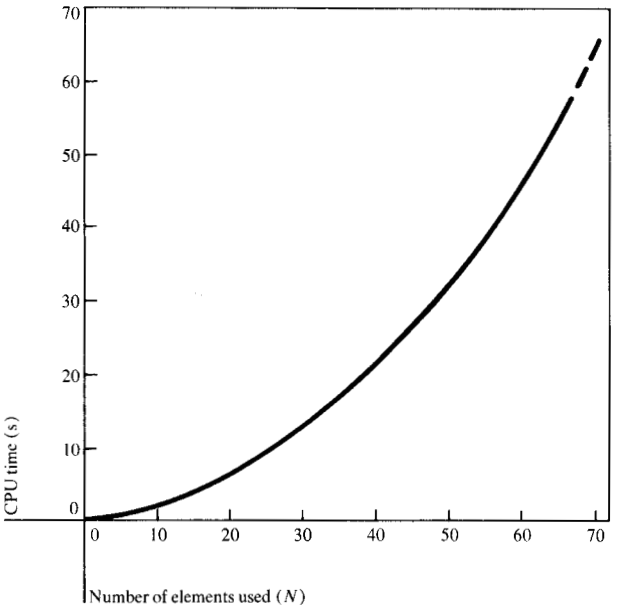

Figure 10 Computation time on an APL system for inversion of $N \times N$ size matrix.

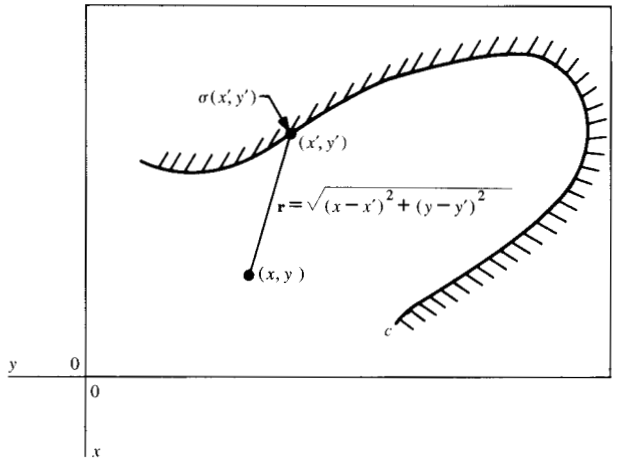

Figure A1 Coordinates for two-dimensional Laplace problems.

of boundary elements. This requires a number of matrix operations including matrix inversion. For example, it took 65 seconds for the APL system on the IBM 370/168 to obtain source charges for a problem whose boundary was divided into 70 segments. Because of this reasonable CPU time, many practical problems can be handled within a day or two, and we have been able to assist practicing engineers with a quick diagnosis of a problem, pointing out a key design parameter in optimization work. Some of the design problems that we have encountered are in the area of stepping motors and print heads used in nonimpact printers.

For the future, we note the proliferation of small portable computer systems having limited workspace but providing plenty of CPU time. In order to adapt the algorithm to such systems, we need to incorporate a mathematical technique such as the matrix partitioning method. This reduces the workspace requirement at the expense of computation time. However, this is not a problem with a standalone system dedicated to one problem at a time. Another area of future work is to extend the algorithm to handle multiple dielectric boundaries and Poisson's equation.

Appendix A: Mathematical formulation

Although the mathematical formulation is fully given elsewhere [12], a review is presented here for completeness and convenience in extending the method to the present application.

The partial differential equation and typical boundary conditions that define the Laplace fields are

$$\nabla^2\phi = 0 \tag{A1}$$

and

$$\alpha\phi + \beta\frac{\partial\phi}{\partial n} = \gamma \tag{A2}$$

along the boundary.

Typically, $\phi(x, y, z)$ represents the field potential and $\nabla\phi(x, y, z)$ the gradient vector with $\partial\phi/\partial n$ indicating the gradient normal to a boundary surface. The boundary condition (A2) includes the Dirichlet condition ($\alpha = 1$, $\beta = 0$), Neumann condition ($\alpha = 0$, $\beta = 1$), and impedance condition ($\alpha = 1$, $\gamma = 0$).

Alternative to (A1), the field can be expressed in an integral form with equivalent boundary sources (or charges). Thus the potential at position vector $\mathbf{r}$ is given by

$$\phi(\mathbf{r}) = \int_s G(\mathbf{r}, \mathbf{r}')\sigma(\mathbf{r}')ds, \tag{A3}$$

where σ is the source (or charge) density along the boundary defined by position vector $\mathbf{r}'$ and G is the kernel or Green's function with the surface integral extending over the whole boundary. In particular, for two-dimensional problems (Fig. A1),

$$\phi(x, y) = \int_c \sigma(x', y') \ln \frac{K}{\sqrt{(x - x')^2 + (y - y')^2}}\, dc, \tag{A4}$$

where K is an arbitrary constant; the primed coordinate system $c = c(x', y')$ traces the boundary for the line integral. The condition imposed in the *a priori* unknown boundary source $\sigma(x', y')$ is that (A4) must satisfy a boundary condition such as (A2).

In general, an exact solution for $\sigma(x', y')$ is not always possible. However, if the line integral is replaced by a Riemann sum, an approximate solution can be obtained in a straightforward manner. To this end, boundary C is first sectioned into $\Delta C_1, \Delta C_2, \cdots, \Delta C$ and, assuming σ is constant over the small subsections (Fig. A2),

$$\phi(x, y) \approx \sum_{i=1}^{N} \sigma_i \int_{\Delta C_i} \ln \frac{K}{\sqrt{(x - x')^2 + (y - y')^2}}\, dc = \sum_{i=1}^{N} \sigma_i \Psi_i(x, y), \tag{A5}$$

where σ_i is the value at the midpoint of ΔC.

Evaluation of line integral

$$\Psi_i(x, y) = \int_{\Delta C_i} \ln \frac{K}{\sqrt{(x - x')^2 + (y - y')^2}}\, dc$$

is achieved through complex variables $z(x, y)$ and function $W(z)$ defined by

$$W_i(z) = \frac{1}{u_i} \int_{z_i}^{z_{i+1}} \ln \frac{K}{z - z'}\, dz' = \frac{1}{u_i} [(z - z_{i+1}) \ln (z - z_{i+1}) - (z - z_i) \ln (z - z_i) + (z_{i+1} - z_i)(1 + \ln K)], \tag{A6}$$

where u_i is the unit vector parallel to ΔC, which extends from z_i to z_{i+1} on the complex z-plane. With the function $W_i(z)$ defined as above, it can be shown that [13]

$$\phi(x, y) = \sum_{i=1}^{N} \sigma_i \Psi_i(x, y) = \sum_{i=1}^{N} \sigma_i \operatorname{Re} [W_i(z)], \tag{A7}$$

where Re [ ] stands for the real part of a complex function. Similarly,

$$\frac{\partial \phi}{\partial x} \approx \sum_{i=1}^{N} \sigma_i \frac{\partial \Psi_i}{\partial x} = \sum_{i=1}^{N} \sigma_i \operatorname{Re} \left[\frac{\partial W_i(z)}{\partial z}\right], \tag{A8}$$

$$\frac{\partial \phi}{\partial y} \approx \sum_{i=1}^{N} \sigma_i \frac{\partial \Psi_i}{\partial y} = \sum_{i=1}^{N} \sigma_i \operatorname{Im} \left[\frac{\partial W_i(z)}{\partial z}\right], \tag{A9}$$

$$\frac{\partial \phi}{\partial n} \approx \sum_{i=1}^{N} \sigma_i \frac{\partial \Psi_i}{\partial n} = \sum_{i=1}^{N} \sigma_i \operatorname{Im} \left[u_i \frac{\partial W_i(z)}{\partial z}\right]. \tag{A10}$$

Here u_i is normal to n as shown in Fig. A2. Im [ ] signifies the imaginary part, and

$$\frac{\partial W_i(z)}{\partial z} = \frac{1}{u_i} \ln \frac{z - z_{i+1}}{z - z_i}. \tag{A11}$$

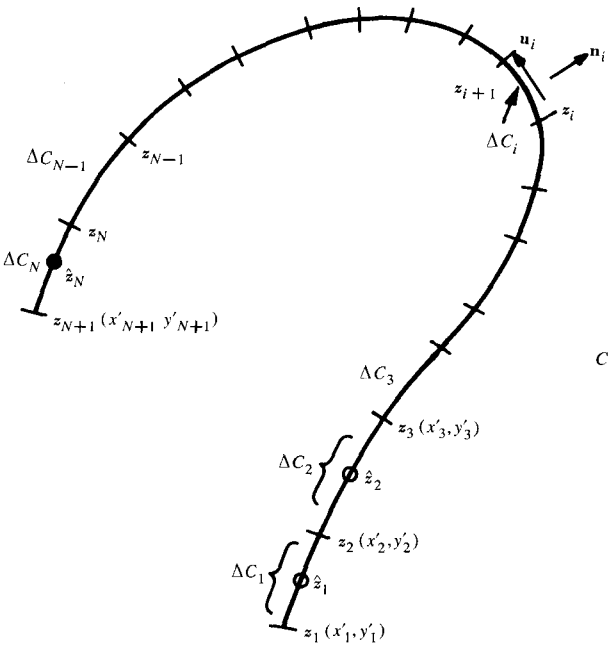

Figure A2 Sectioned boundary on complex plane.

The boundary condition (A2), when rewritten for the sectioned boundaries, is

$$\alpha_i \phi_i + \beta_i \frac{\partial \phi_i}{\partial n} = \gamma_i \qquad i = 1, 2, \cdots, N, \tag{A12}$$

where $\phi_i = \phi(\hat{z}_i)$, and $\hat{z}_i$ is the midpoint of ΔC_i or $\hat{z}_i = 1/2(z_i + z_{i+1})$. Thus, the source σ_i's are determined approximately by substituting (A5) or (A7) and (A10) into (A12), giving

$$\alpha_i \left[\sum_{j=1}^{N} \sigma_j \Psi_j(\hat{z}_i)\right] + \beta_i \left[\sum_{j=1}^{N} \sigma_j \frac{\partial \Psi^i}{\partial n}(\hat{z}_i)\right] = \gamma_i, \tag{A13}$$

or

$$\sum_{j=1}^{N} \left[\alpha_i \Psi_j(z_i) + \beta_i \frac{\partial \Psi^j}{\partial n}(z_i)\right] \sigma_j = \gamma_i \qquad i = 1, 2, \cdots, N; \tag{A14}$$

or, in matrix form,

$$[\ell]\bar{\sigma} = \bar{\gamma} \text{ or}$$

$$\bar{\sigma} = [\ell]^{-1}\bar{\gamma}, \tag{A15}$$

where

$$\ell_{ij} = \alpha_i \Psi_j(\hat{z}_i) + \beta_i \frac{\partial \Psi^j}{\partial n}(\hat{z}_i), \tag{A16}$$

$$\Psi_j(\hat{z}_i) = \operatorname{Re} [W_j(\hat{z}_i)], \tag{A17}$$

$$\frac{\partial \Psi_j(\hat{z}_i)}{\partial n} = \operatorname{Im} \left[u_i \frac{\partial W_j(\hat{z}_i)}{\partial z}\right] \qquad i = 1, 2, \cdots, N. \tag{A18}$$

The terms $\bar{\sigma}$ and $\bar{\gamma}$ are column matrices $(\sigma_1, \sigma_2, \cdots, \sigma_N)$ and $(\gamma_1, \gamma_2, \cdots, \gamma_N)$, respectively. The complex functions W_j and, $\partial W_j/\partial z$ are given by (A6) and (A11) and it is noteworthy that

$$W_j(\hat{z}_i) = W\{\hat{z}; z_j, z_{j+1}\}, \tag{A19}$$

$$\frac{\partial W_j}{\partial z}(\hat{z}_i) = \frac{\partial W}{\partial z}\{\hat{z}_i; z_j, z_{j+1}\}, \tag{A20}$$

$$\ell_{ij} = \ell\{\hat{z}_i; z_j, z_{j+1}\}. \tag{A21}$$

Once σ_j's have been determined, the potential ϕ and gradients $\partial\phi/\partial x$ and $\partial\phi/\partial y$ are obtained from (A7), (A8), and (A9).

The above formulation has been incorporated into a set of compact APL programs which cover a broad range of two-dimensional problems with arbitrary boundaries [10].

References

1. Albert E. Ruehli, "Survey of Computer-Aided Electrical Analysis of Integrated Circuit Interconnections," *IBM J. Res. Develop.* **23,** 626-639 (1979).
2. C. M. Sakkas, "Potential Distribution and Multi-Terminal DC Resistance Computations for LSI Technology," *IBM J. Res Develop.* **23,** 640-651 (1979).
3. W. T. Weeks, "Exploiting Symmetry in Electrical Packaging Analysis," *IBM J. Res. Develop.* **23,** 669-674 (1979).
4. Clive Temperton, "Direct Methods for the Solution of the Discrete Poisson Equation: Some Comparisons," *J. Comput. Phys.* **31,** 1-20 (1979).
5. R. W. Hockney, "The Potential Calculation and Some Applications," *Methods of Computational Physics*, B. Alder, S. Fernbach, and M. Rotenberg, Eds., Academic Press, Inc., New York, 1969, Vol. 9, pp. 135-211.
6. B. L. Buzbee, F. W. Dorr, J. A. George, and G. H. Golub, "The Direct Solution of the Discrete Poisson Equation on Irregular Regions," *SIAM J. Numer. Anal.* **8,** 722-736 (1971).
7. F. B. Hildebrand, *Methods of Applied Mathematics*, 2nd Ed., Prentice-Hall, Inc., Englewood Cliffs, NJ, 1965, Ch. 3.
8. Roger F. Harrington, *Field Computation by Moment Method*, The Macmillan Co., New York, 1968.
9. H. D. Chai, "Technique for Finding Permeance of Tooth Structures of Arbitrary Geometry," *Proceedings of International Conference on Stepping Motors and Systems*, University of Leeds, England, July 13-15, 1976.
10. H. D. Chai and H. C. Lee, "An APL Algorithm for Two-Dimensional Laplace Problems Using the Moment Method," *Technical Report TR 01.2222*, IBM System Products Division laboratory, Endicott, NY, 1974.
11. L. Gilman and A. J. Rose, *APL: An Interactive Approach*, 2nd Edition, John Wiley & Sons, Inc., New York, 1974.
12. R. F. Harrington, K. Pontoppidan, P. Abrahamsen, and N. C. Albertsen, "Computation of Laplacian Potentials by an Equivalent Source Method," *Proc. IEEE* **116,** 1715-1720 (1969).
13. E. Weber, *Electromagnetic Fields Theory and Applications*, John Wiley & Sons, Inc., New York, 1950.

Received September 19, 1979; revised April 24, 1980

The authors are located at the IBM System Products Division laboratory, P.O. Box 6, Endicott, New York 13760.